Synthesis and properties of [Pt(4-CO2CH3-py)2(mnt)]: Comparison of pyridyl and bipyridyl-based dyes for solar cells

Post-print of a peer-reviewed article published by the Royal Society of Chemistry.
Published article available at: http://dx.doi.org/10.1039/B811943K

Cite as:
Moorcraft, L. P., Morandeira, A., Durrant, J. R., Jennings, J. R., Peter, L. M., Parsons, S., Turner, A., Yellowlees, L. J., & Robertson, N. (2008). Synthesis and properties of [Pt(4-CO_2CH_3-py)$_2$(mnt)]: Comparison of pyridyl and bipyridyl-based dyes for solar cells. *Dalton Transactions*, (48), 6940-6947.

Manuscript received: 14/07/2008; Accepted: 08/09/2008; Article published: 03/11/2008

Synthesis and properties of [Pt(4-CO_2CH_3-py)$_2$(mnt)]: Comparison of pyridyl and bipyridyl-based dyes for solar cells**

Lucy P. Moorcraft,[1] Ana Morandeira,[2] James R. Durrant,[2] James R. Jennings,[3] Laurence M. Peter,[3] Simon Parsons,[1] Andrew Turner,[1] Lesley J. Yellowlees,[1] Neil Robertson[1,*]

[1]EaStCHEM, School of Chemistry, Joseph Black Building, University of Edinburgh, West Mains Road, Edinburgh, EH9 3JJ, UK.

[2]Centre for Electronic Materials and Devices, Department of Chemistry, Imperial College, London, UK.

[3]Department of Chemistry, University of Bath, Bath, UK.

[*]Corresponding author; e-mail: neil.robertson@ed.ac.uk; fax: +44 1316 504743 ; tel: +44 1316 504755

[**]We thank Donald Robertson for providing Na_2mnt and Johnson Matthey for the supply of $K_2[PtCl_4]$ for use in this study. Financial support from EPSRC under the Supergen Excitonic Solar Cells project is gratefully acknowledged. This work has made use of the resources provided by the EaStCHEM Research Computing Facility. (http://www.eastchem.ac.uk/rcf). This facility is partially supported by the eDIKT initiative (http://www.edikt.org).

Supporting information:
[†]Electronic supplementary information (ESI) available: Fig. S1, CV of 1b; Fig. S2, CV of 2b; Fig. S3 and Table S1, OTTLE of 1b; Fig. S4 and Table S2, OTTLE of 2b; Fig. S5, EPR spectrum and simulation of 1b1−; Table S3, EPR simulation parameters for 1b1−; Fig. S6, EPR spectrum and simulation of 2b2−; Table S4, calculated atom contributions to frontier orbitals of 3b and Table S5, TDDFT calculated selected transitions for 3b. CCDC reference number 694836. For ESI and crystallographic data in CIF or other electronic format see http://dx.doi.org/10.1039/B811943K

Abstract

The dye complexes [Pt(4-CO_2R-py)$_2$(mnt)] (R = H (**3a**), CH_3 (**3b**)) and the precursor complexes [Pt(4-CO_2R-py)$_2$$Cl_2$] (**2a**, **2b**) (py = pyridyl) were synthesised, characterised by electrochemical, spectroscopic, spectroelectrochemical (UV/Vis/nIR and *in situ* EPR) and hybrid DFT computational methods and attached to a TiO_2 substrate to determine charge recombination kinetics. The results were compared to the bipyridyl analogues [Pt{X,X'-(CO_2R)-2,2'-bipyridyl}(mnt)], (X = 3 or 4). The electronic characteristics of the bis-pyridyl complex were found to be different to the bipyridyl complexes making the former harder to reduce, shifting the lowest-energy absorption band to higher energy and showing separate degenerate LUMO orbitals on the two pyridine rings. The latter point determines that the direduced pyridyl complex remains EPR active unlike the bipyridyl analogue. Complex **3a** attached to nanocrystalline TiO_2 shows a long charge recombination lifetime in comparison with the analogous complex with the ubiquitous 4,4'-(CO_2H)$_2$-bipyridyl ligand, suggesting that pyridyl complexes may possess some advantage over bipyridyl complexes in dye-sensitised solar cells.

Introduction

Square planar d^8 [Pt(II)(diimine)(dithiolate)] complexes have attracted much attention due to their attractive electronic and photochemical properties.[1a,b] They are known to show luminescence in fluid solution at ambient temperatures and absorb in the visible region with extinction coefficients ε of 5000 – 10000 $M^{-1}cm^{-1}$. This solvatochromatic visible absorption has been described as a "mixed-metal-ligand-to-ligand" charge transfer (MMLL'CT) due to the significant metal character in the dithiolate-based HOMO and has been assigned as a (Pt(d)/S(p)/dithiolate → π*/diimine) transition which typically appears around 450-500nm.[1a]

Research on a series of [Pt(II)(diimine)(dithiolate)] complexes by Eisenberg and co-workers has shown that systematic modifications to one or both of the ligands can predictably alter the excited state energies by up to 1eV.[1a] The assignment of the HOMO as mostly dithiolate based and the LUMO as diimine based allowed the separate tuning of either of these orbitals to achieve the desired photophysical characteristics. This has been exploited for example in light harvesting for photochemical hydrogen production[2] and non-linear optical studies.[3] Related complexes have also been prepared where the dithiolate is replaced by two monodentate thiolate ligands.[4]

The high tunability and good photoluminescent properties of [Pt(II)(diimine)(dithiolate)] complexes also mean that they are good candidates for sensitising dyes in DSSCs. In 1991 O'Regan and Grätzel reported the design of the dye-sensitised solar cell (DSSC) which has since shown power conversion efficiencies of up to 11%.[5] These cells consist of dye molecules, anchored to the surface of nanocrystalline TiO_2, which absorb visible light and inject an electron into the conduction band of the TiO_2 from their excited state. The dye is re-

reduced by a solution redox couple and the separated electrons and holes are collected at different electrodes to produce the cell potential.

The tunability of [Pt(II)(diimine)(dithiolate)] complexes makes them excellent model dyes for studies of the light-harvesting and electron transfer processes since the HOMO and the LUMO characteristics can each be separately altered. The tuning of the HOMO by varying the dithiolate ligand has been investigated[6,7] and tuning the LUMO has been achieved by us through study of a family of [Pt(II)(diimine)(dithiolate)] complexes with the general formula [Pt{X,X'-(CO_2R)-2,2'-bipyridyl}(mnt)] (where X = 3, 4, or 5, R = H or Et and mnt = maleonitriledithiolate).[8] For these complexes, alteration of the position of attachment of the carboxylic acid group is of particular importance as this controls the electronic coupling with the TiO_2 and the interfacial electron transfer processes that drive the solar cell. The 3,3' analogue was found to give the best cell performance of the series, despite the fact that studies of metal-bipyridyl dyes have almost entirely focussed on 4,4'-(CO_2H)-bpy ligands (bpy = bipyridyl). This was due to more favourable (i.e. slower) charge-recombination kinetics than for the 4,4' and 5,5' analogues. A twist which disrupts the planarity of the bipyridine in the 3,3'-dye was interpreted as the origin of this improved performance as the reduced delocalisation inhibits the charge recombination.[9]

This observation has now led us to investigate substituted pyridines (hereafter abbreviated as py) as ligands in such square-planar Pt complexes instead of the bpy moiety since this will lead to further decoupling of the two pyridyl rings. Despite the intense interest in the related [Pt(II)(diimine)(dithiolate)] complexes, only one prior study of a [Pt(II)($py)_2$(dithiolate)] complex, [Pt(4-CH_3-$py)_2$(mnt)], has previously been reported however in this case the electronic properties have not been thoroughly studied.[10] Pyridyl ligands have occasionally been used in Ruthenium DSSC sensitisers[11-14] but have not been widely investigated. They could offer flexible synthetic options and tunability of the absorption spectrum for a dye as well as possibly higher molar extinction coefficients than analogous bpy complexes.[15] Here we report the synthesis, electronic characterisation and charge recombination kinetics for the substituted-pyridine complex [Pt(II)(4-CO_2CH_3-$py)_2$(mnt)] along with the precursor complexes, representing the first detailed electronic characterisation of a [Pt(II)($py)_2$(dithiolate)] complex.

Results and Discussion

Synthesis and Structure

[Pt(4-CO_2CH_3-$py)_2$mnt] **3b** was synthesised using the route shown in Scheme 1. Reaction of two molar equivalents of 4-CO_2CH_3-py with potassium tetrachloroplatinate gave the dichloro-substituted platinum precursor **2b** and further reaction of this compound with the disodium salt of mnt gave the desired product. This was based on a similar procedure to that for the synthesis of the bipyridine analogues (**4b**, **5b**), except

that the pyridyl complexes were more susceptible to degradation during isolation, presumably due to greater lability of the monodentate ligands and care had to be taken to avoid heating during workup.

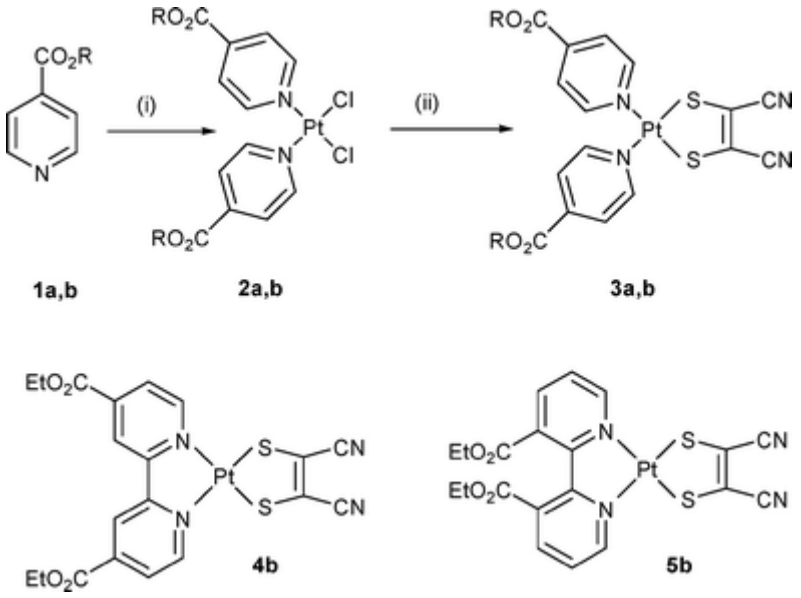

Scheme 1. Synthesis of [Pt(4-CO_2R-py)$_2$(mnt)] **3**, where R = H **3a** or CH_3 **3b**. (i) $K_2PtCl_{4(aq)}$, reflux (ii) Na_2mnt, RT. Related bipyridyl complexes that we have previously reported,[8,9] **4b** and **5b**, are shown for comparison.

Both acid and ester analogues of the dichloride and the mnt complex were prepared. The acid species are more appropriate for easy binding to TiO_2, whereas the ester analogues show greater solubility in a wider range of solvents and produce clearer results in the electrochemical characterisation techniques used.

Although no crystal structure of [Pt(4-CO_2CH_3-py)$_2$mnt] was obtained, the crystal structure of the dichloride complex **2b** was determined (Fig. 1) and, due to its *cis*-structure, is expected to show similar features to **3b** regarding the pyridyl units. The molecule resides on a two-fold axis and the Pt-N bond length (2.018(2) Å) and Pt-Cl bond length (2.2976(6) Å) are within the normal range for Pt(II) square-planar species.[16] The planarity of the Pt centre is verified by angles of ~90° between neighbouring groups and ~180° between opposite groups. The torsion angle N1-Pt-N1-C2 is 80.55º such that both pyridyl ligands are almost orthogonal with the platinum dichloride plane and also with each other. This is shown by the angle between the planes formed between the C_5N-rings of the two pyridyl ligands which is 86.69°. The complex has *cis* geometry as would be expected from the *trans* effect directed substitution of $[PtCl_4]^{2-}$ and this geometry might aid the subsequent addition of the bidentate dithiolate ligand. Twenty-one [Pt(substituted-pyridyl)$_2$Cl$_2$] complexes have been structurally characterised[16] to date, however only five of these showed *cis* geometry. Only one of these structures contains pyridines substituted with esters in the 4-positions and this showed *trans*

geometry.[17] To compare, the Pt-N bonds in the crystal structure of [Pt{3,3'($CO_2CH_2CH_3$)$_2$-2,2'-bipyridyl}(mnt)] **5b** are slightly longer than for the pyridine complex at 2.074(10) and 2.058(8) Å and the N-Pt-N angle is much narrower at 79.4(3)º.[8] This illustrates the compromise introduced by the inflexibility of the bpy ligand in comparison with two pyridyl ligands.

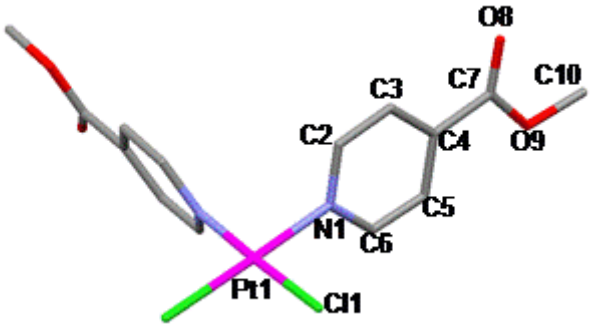

Figure 1. Crystal Structure of [$PtCl_2$(4-CO_2CH_3-py)$_2$] 2**b** with H atoms removed for clarity. Selected bond lengths (Å) and angles (º): Pt-Cl(1) 2.2967(6); Pt-N(1) 2.018(2); N(1)-Pt-N(1) 88.91(11); Cl(1)-Pt-Cl(1) 92.32(3); N(1)-Pt-Cl(1) 89.39(6), 178.20(6).

Electrochemistry

The electrochemistry of [Pt(4-CO_2Me-py)$_2$(mnt)] **3b** was studied by cyclic voltammetry (in a solution of 0.1M $TBABF_4$/DMF) (Fig. 2, Table 1) and shows two reversible (as evidenced by straight line plots of i_{max} vs (scan rate)$^{1/2}$) reduction peaks at -1.10 V and -1.25 V and a chemically-irreversible oxidation at 1.24 V. The electrochemistry of the related platinum dichloride complex **2b** (Fig. S2†), also shows two reversible reductions at very similar potential. These processes are therefore assigned as sequential reductions based on the two substituted-pyridyl ligands. The absence of any oxidation for **2b** enables the oxidation at 1.24 V for **3b** to be assigned as based on the mnt ligand.

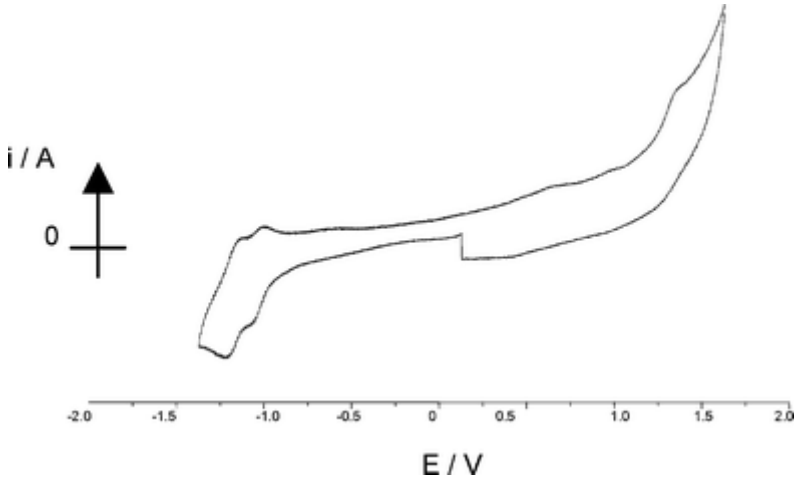

Figure 2. Cyclic voltammetry of [Pt(4-CO_2CH_3-py)$_2$mnt] **3b** in 0.1 M $TBABF_4$ / DMF at 298 K, Scan rate 0.1 V s^{-1}.

Table 1. Electrochemical data ($E_{1/2}$) recorded in DMF/0.1 M $TBABF_4$ versus Ag/AgCl. *chemically-irreversible process

	E^{ox}	$E^{red(1)}$	$E^{red(2)}$	$E^{red(1)}$-$E^{red(2)}$
1b	-	-1.69	-	-
2b	-	-1.15	-1.32	0.17
3b	+1.24*	-1.10	-1.25	0.15
4b[8,9]	+1.39*	-0.65	-1.20	0.55
5b[8,9]	+1.35*	-0.59	-12.0	0.61

For a dye to be viable within the energetics of a TiO_2 DSSC, the first reduction must be sufficiently negative to inject an excited-state electron into the titania conduction band and the process at -1.10 V shows that this is the case for **3b,** as well as the excited-state electron being positioned on the pyridyl, appropriate for rapid injection into the band via the carboxy groups that bind to TiO_2. The first oxidation of **3b** is sufficiently positive to be rapidly reduced by the I^-/I_3^- redox electrolyte within the cell.

The analogous bipyridine complexes **4b** and **5b** also show two electrochemically-reversible reductions, based on the bipyridine ligand, and an irreversible oxidation based on the mnt ligand.[8,9] The first reduction of the substituted pyridyl complex **3b** is at more negative potential than the first reduction of the bipyridyl complexes as there is less delocalisation within the pyridyl ligands to stabilise the addition of an extra electron. It is also very striking that the separation of the first and second reductions for the bpy-complexes is much greater than for **2b** or **3b**, indicating the substantial pairing energy required to add two electrons to one orbital of the bpy in comparison with adding one electron to each pyridyl-ligand of **2b** or **3b**. This is discussed further in subsequent sections. The separation between the first oxidation and the first reduction for **3b** is 2.34 V compared to 2.04 V for **4b**. This reflects the poorer electron accepting ability of the pyridyl ligands and means that the absorption wavelength of the pyridine complex is expected to shift to shorter wavelength.

Hybrid DFT calculations on [Pt(4-CO_2CH_3-py)$_2$(mnt)] **3b** (Fig. 3, Table S4[†]) show that the HOMO is based mostly on the dithiolate ligand. Similar to **4b** and **5b**, this orbital has some mixed-metal contribution to the orbital with 14.4 % platinum character. The LUMO is based on the substituted pyridine part of the molecule, with only 3.2% platinum character, agreeing with the cyclic voltammetry, UV/Vis and EPR results (see below) that also indicate the LUMO is pyridine-ligand based. Some complication in the calculation was observed regarding the distribution of the LUMO over the pyridyl ligands. Two, essentially degenerate LUMO orbitals are determined (the energies of these two orbitals are very close and within the limits of the calculation may be regarded as degenerate), however the extent to which these spread over the two pyridyl ligands depends upon the angle between these. Restricting the geometry of the pyridine ligands in **3b** to a torsion angle of 90° in relation to one another (similar to the torsion angle seen in the crystal structure of 2**b**) caused each LUMO to be based almost entirely on only one each of the pyridine ligands rather than being

spread over both (See Fig. 3). This is then in agreement with the experimental observation by EPR that the unpaired electron in the SOMO is based only on one pyridine ligand (see below).

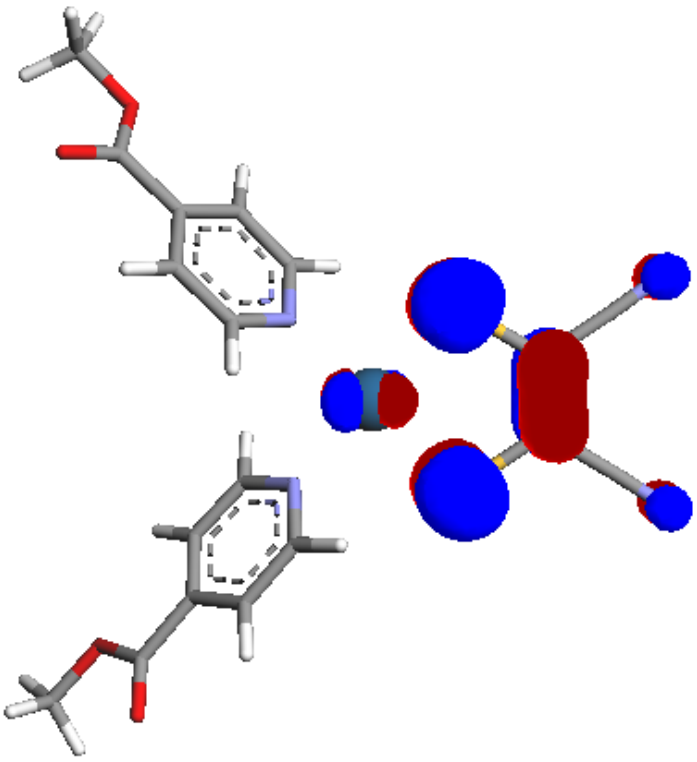

Figure 3. HOMO (left) and LUMO (right) isosurfaces for [Pt(4-CO_2CH_3-py)$_2$(mnt)]. Individual atom contribution can be found in Table S4†.

TD-DFT calculations were carried out on **3b** in the presence of DMF. This method has previously been demonstrated to give satisfactory results for [Pt(diimine)(dithiolate)] systems and is therefore expected to be applicable also to [Pt(py)$_2$(dithiolate)] complexes.[9,18,19] A summary of relevant calculated transitions for **3b** can be found in Table S5† and the calculated transitions relative to the observed absorption spectrum are shown in Fig. 4. It should be noted that the inclusion of solvent in these calculations was undertaken as it has been observed previously that TD-DFT studies carried out in vacuum typically vastly underestimated the energy of the lowest energy transition in related complexes.[9]

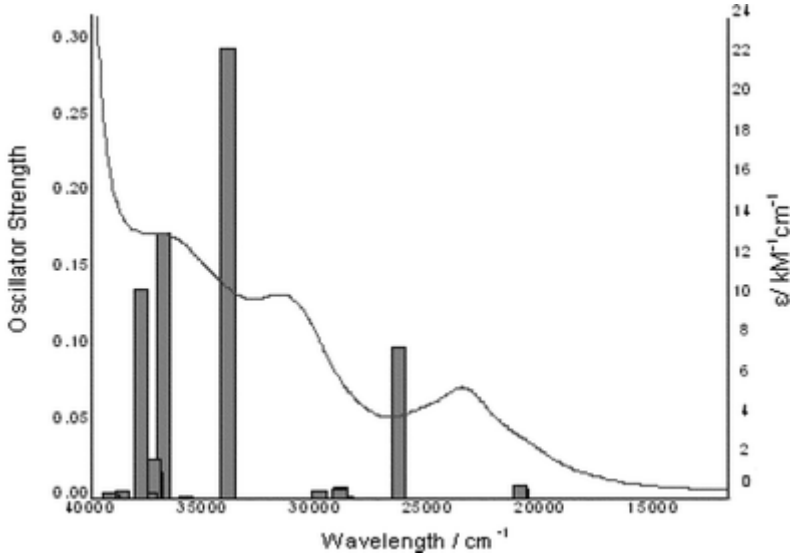

Figure 4. Calculated TD-DFT results of **3b** shown as bar chart (left axis) relative to the observed absorption spectrum (right axis) in DMF.

Only four transitions with significant oscillator strength (>0.1) were found and these correlate reasonably well with the spectrum of **3b**, which has absorptions at 36300 cm^{-1}, 31600 cm^{-1} and 25700 cm^{-1}. The lowest energy band for **3b** does not occur in either **1b** or **2b** consistent with assignment as ligand-to-ligand charge transfer (LLCT), analogous to the lowest energy transition in the bpy-species **4b** and **5b**. The calculated composition was found to be 76% HOMO-LUMO+2, which interestingly does not involve the lowest energy degenerate LUMO orbitals on the pyridyl ligands but instead the next-highest energy orbital, which is also pyridyl based. The calculated energy is slightly overestimated, by 611 cm^{-1}.

The two higher energy peaks show a marked similarity to those displayed by the dichloride analogue **2b** (Figure S4[†]) which has transitions at 35600 cm^{-1} and at 30200 cm^{-1}. Although a $\pi \rightarrow \pi^*$ absorption at 36500 cm^{-1} was observed for the ligand **1b**, it was of lower intensity than the 36300 cm^{-1} band of **3b** suggesting the latter has some other character. This was confirmed by the calculations on **3b** showing this band to be charge transfer in character from HOMO-3 (49% Pt, 46% mnt-based) to LUMO (80% py-based). The lower-energy process (31600, 30200 cm^{-1} for **3b**, **2b** respectively) also has no equivalent transition in **1b** and is also shown to be charge-transfer in nature for **3b** from HOMO-1 (32% Pt, 52% S) to LUMO+2.

The relative size of the oscillator strengths match the relative intensities of the observed spectra well, taking into account the presence of two significant transitions under the band at 36300 cm^{-1}.

The LLCT in the neutral complex is observed at the onset of the visible region at 25700 cm^{-1} (390 nm). This is rather high energy for use in a solar cell as dyes with absorption maximum of around 550 nm are more typical. This reflects the combination of the pyridyl ligands with a dithiolate ligand (mnt^{2-}) that leads to a very positive

oxidation potential for the dyes and further tuning of the dithiolate ligand will readily allow absorption at a more optimised region of the visible spectrum.

The neutral bipyridine analgogue **4b** shows similar peaks to **3b** around the 30000 cm^{-1} region which are assigned to $\pi \rightarrow \pi^*$ transitions. There is also a LLCT transition at 18900 cm^{-1}, at a lower energy than in the pyridine analogue, which fits well with the larger oxidation – reduction energy gap seen in the electrochemistry of **3b** compared with **4b**.

Spectroelectrochemistry and EPR

UV/Vis/NIR spectroelectrochemistry (Fig. 5) was performed to gain further information on the frontier orbitals of [Pt(4-CO_2CH_3-py)$_2$mnt]. This involved electrochemical reduction of this compound to its mono- and di-reduced and oxidation to its mono-oxidised states. Comparison with related studies for **1b** and **2b** (Fig. S3,S4; Table S1,S2[†]) gave some insight into the absorption processes.

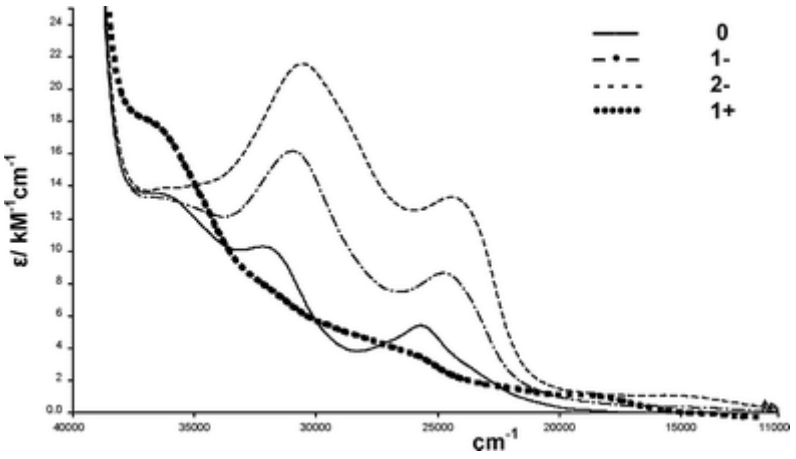

Figure 5. UV/vis/NIR of **3b** in 0, -1, -2 and +1 oxidation states. Spectra were run in 0.1M $TBABF_4$/DMF at 233 K. E_{gen} = 0 V (0), -1.3 V (-1), -1.6 V (-2) and 1.5 V (+1). The spectrum was observed to stabilise at -1.3 V before undergoing further change at -1.6 V indicating sequential reduction to mono then dianion.

Reduction to $\mathbf{3b}^{1-}$ and $\mathbf{3b}^{2-}$ retains the peak at 36300 cm^{-1}, while the 31600 cm^{-1} peak and lower energy LLCT band increase in intensity and shift slightly to lower energy. These spectra show marked similarities to that of

the reduced dichloride precursor **2b**$^{1-/2-}$ supporting the conclusion that the reduction electrons enter the 4-CO_2CH_3-py based orbitals. Reducing from the mono- to di-reduced compound, the spectrum simply shows an increase in intensity of the bands rather than formation of new ones, consistent with sequential reduction of the pyridyl ligands with very little interaction between them. This contrasts greatly with **4b**$^{2-}$ where the lowest energy HOMO-LUMO transition of the neutral species **4b** is completely lost due to filling of the LUMO orbital.

Upon oxidation to [Pt(4-CO_2CH_3-py)$_2$(mnt)]$^+$ there is an increase in intensity at 36300 cm^{-1}, a decrease in intensity at 31600 cm^{-1} and 25700 cm^{-1} and a further peak at 18500 cm^{-1} grows in. Despite the irrevesibility of the oxidation in the CV, at the reduced temperature of the spectroelectrochemistry experiment this process was chemically reversible.

In situ EPR study of [Pt(4-CO_2CH_3-py)$_2$(mnt)]$^{2-}$ (Fig. 6) shows coupling constants to the Pt (II) metal centre and the N nuclei of 41 G and 6.7 G respectively. Coupling to other ligand nuclei are unresolved due to the large linewidth required to successfully simulate the spectrum. In comparison with the analogous dichloride complex **2b**$^{2-}$ (Fig. S6†), the coupling value to the nitrogen atom is unchanged but the electron no longer couples as strongly to the platinum centre, with coupling reduced from 55.5 G to 41 G (Table 2). This result confirms that the LUMO is based on the pyridine moiety. As less coupling is seen to the platinum centre than in the dichloride precursor, this suggests that the orbital is more delocalised once the mnt ligand has been attached. A reduction in coupling to the platinum from the dichloride precursor (59.5 G) to the mnt complex (56.0 G) was also seen with the bpy complex analogues,[9] also suggesting greater electronic delocalization once the mnt ligand is attached. Coupling to N was larger in **2b** and **3b** than in the uncomplexed species **1b** (Table S3) suggesting some polarisation of the spin density toward the nitrogens when complexed to the Pt centre.

Table 2. EPR Simulation Parameters for **2b**$^{2-}$(spectrum shown in Fig. S6†) and **3b**$^{2-}$ in 0.1 M $TBABF_4$ in DMF at 233 K. All hyperfine coupling constants given in G. Δ = linewidth. g = Landé g-factor.

Parameter	**2b**$^{2-}$	**3b**$^{2-}$
a_{iso}(Pt)	55.5	41
a_{iso}(N)	6.7	6.725
g	2.0003	2.0043
Δ	5.75	5.5

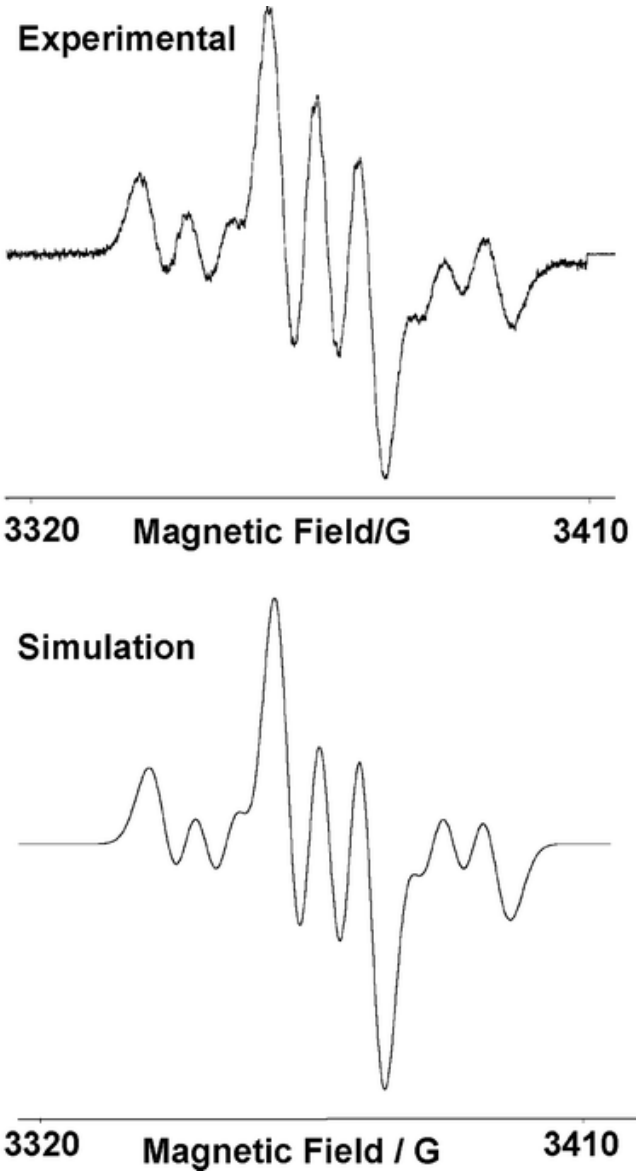

Figure 6. EPR spectrum and simulation of $\mathbf{3b}^{2-}$. Spectrum was run in 0.1M $TBABF_4$/DMF at 233K. E_{gen} = -1.4 V.

Two key differences arise in the EPR spectra of the reduced forms of **3b** in comparison with **4b**. Firstly, for $\mathbf{4b}^{2-}$ the signal collapses when the second electron is added as it enters the same orbital as the first reduction electron and gives diamagnetic properties. Holding the pyridine analogue $\mathbf{3b}^{2-}$ at very negative potentials however does not result in a decrease in signal suggesting that electrons enter two different orbitals (one on each pyridine ligand) and can not pair up. Secondly, for $\mathbf{4b}^{1-}$ the electron couples to two nitrogens whereas coupling to only one nitrogen atom is seen for $\mathbf{3b}^{1-/2-}$ again demonstrating the confinement of the radical to one pyridyl ligand for the latter.

Kinetics of electron transfer on TiO_2

One of the goals for the synthesis of this class of complex was as a model system to assess the potential of pyridyl dyes in dye-sensitised solar cells. Our previous observations on **4a** and **5a** demonstrated[8,9] that the twist in the bipyridyl for **5a** leads to slower charge recombination and better solar cell performance. We wished therefore to determine whether complete separation of the two rings into separate pyridyl ligands would reproduce the favourable charge-recombination kinetics of **5a**. We therefore determined, using transient-absorption spectroscopy, the charge-recombination lifetimes for **3a** and **5a** using the same experimental conditions to ensure the results would be comparable. This was achieved by sensitisation of TiO_2 using **3b** and **5b** hydrolysed *in situ* and appended to nanocrystalline TiO_2. Following excitation and injection of excited state electrons into the TiO_2 conduction band, the charge recombination was followed by monitoring the decay at 990 nm where electrons in the TiO_2 conduction bands are known to absorb. The observed dynamics could be well reproduced by single exponential functions with charge recombination time constants of 30 and 40 ms for **3a** and **5a**, respectively (Fig. 7).

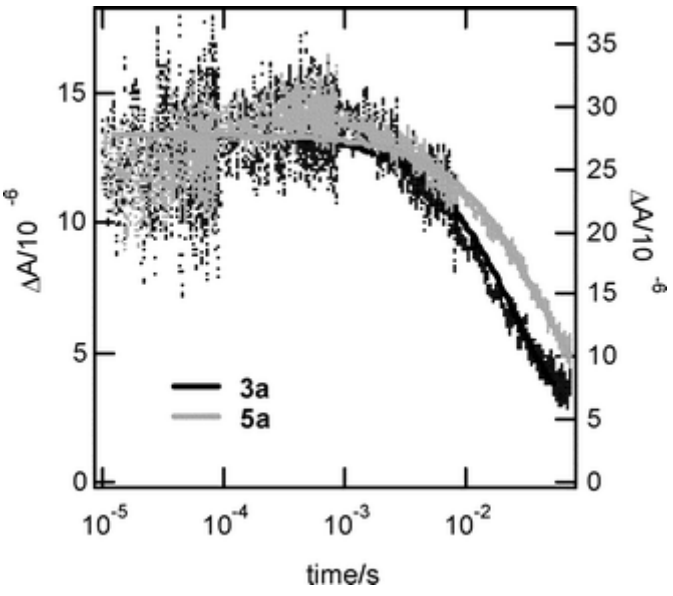

Figure 7. Transient absorption data monitoring the charge recombination kinetics for TiO_2 film sensitised with [Pt(4-CO_2CH_3-py)$_2$(mnt)] (**3a,** dotted black, left axis) and [Pt{3,3'-($CO_2CH_2CH_3$)$_2$-2,2'-bpy}(mnt)] (**5a**, dotted gray, right axis). The solid lines are single exponential fits of the data. The excitation wavelengths are 450 nm and 530 nm for **3a** and **5a**, respectively. At those wavelenths, the amount of photons absorbed by each dye was comparable. The probe wavelength is 990 nm in both cases.

These lifetimes are of the same order of magnitude and very similar in absolute value. This demonstrates that substituting the twisted, 3,3'-substituted bipyridine ligand with two completely-separated pyridine ligands has retained the slow recombination kinetics seen in the 3,3'-substituted ligand. It should be noted that the very-commonly used ligand in dye-sensitsed solar cells is the 4,4'-(CO_2H)-bpy ligand present is **4a** which has already shown faster charge recombination that **5a** and hence also faster than **3a**. Thus we have established that the pyridyl complex displays superior charge-recombination kinetics to the analogous complex with this common ligand. In addition, we have also provided some additional clarity for the superior performance of **5a** over **4a** where the twist in the bpy ligand and associated loss of delocalisation appears to play a key role.

Conclusions

This study has demonstrated the first electronic characterisation of a complex of type [$Pt(py)_2$(dithiolate)], analogues of the much-studied [Pt(bpy)(dithiolate)] family of complexes. Electrochemical, spectroelectrochemical, EPR and computational results all consistently showed the lack of communication between the two pyridyl rings and that the di-reduced species involves one electron on each pyridyl. This contrasts greatly with the bpy-analogues and is the principal electronic difference between the two series of complexes. The poorer electron accepting ability of the pyridyl leads to blue-shifting of the lowest energy transition of the complex, which was mainly of HOMO-LUMO+2 character, and a shift of the first reduction potential to more negative value.

In the context of solar cell dyes, we found that replacing a bipyridine ligand substituted in the 3,3'-positions in a solar cell dye with two pyridines is likely to lead to comparable charge-separated lifetime for injected electrons in TiO_2. Since we have already demonstrated superior charge-separated lifetime for 3,3'-$(CO_2H)_2$-bpy containing dyes on TiO_2 compared with the ubiquitous 4,4'-$(CO_2H)_2$-bpy containing dyes, the current work also demonstrates that pyridyl-containing dyes may share these advantages. Subsequent work will involve the application of these concepts to Ru-complex dyes that typically give higher efficiencies in DSSC. It is interesting to note that Ru complexes with pyridyl ligands have also been shown in some cases to give higher absorption coefficients than those with analogous bpy ligands.[15] Taken together with the possibility of favourable charge- recombination kinetics, pyridyl ligands may deserve greater consideration in dyes for DSSC than they have received until now.

Experimental Section

Methyl isonicotinate (4-CO_2CH_3-py), purchased from Sigma-Aldrich/Fluka and K_2PtCl_4 provided by Johnson Matthey were used as received. Na_2(mnt) was prepared as previously reported.[20]

Synthesis of [$PtCl_2$(4-CO_2CH_3-py)$_2$] (**2b**). $K_2[PtCl_4]$ (198.4 mg, 0.478 mmol) and 4-CO_2CH_3-py (130.3 mg, 0.951 mmol) were refluxed in deionised water (50 mL) for one hour. The yellow precipitate was filtered, washed with diethyl ether and then dried in a vacuum. The solid was recrystallised from a hot saturated solution of DMF. Yield: 82 % (212 mg, 0.392 mmol); MS (FABMS), *m/z*: 540 $\{M\}^+$ also peaks at 505 $\{M\text{-}Cl\}^+$, 468 $\{M\text{-}2Cl\}^+$; Anal. Calcd for $PtCl_2N_2O_4C_{14}H_{14}$: C, 31.11; H, 2.59; N, 5.19. Found C, 31.02; H, 2.61; N, 5.02*;* ^{1}H NMR (250 MHz, $CDCl_3$): δ 4.0 (6H, s), δ7.8 (4H, d), δ8.9 (4H, d). IR (KBr, cm^{-1}): 1729 (s) (C═O stretch).

Synthesis of [$PtCl_2$(4-CO_2H-py)$_2$] (**2a**). $K_2[PtCl_4]$ (203.4 mg, 0.49 mmol) and 4-CO_2H-py (114.9 mg, 0.934 mmol) were refluxed in deionised water (50 mL) for one hour. The water was then removed *in vacuo* to leave a yellow solid and recrystallised from a hot saturated solution of DMF. Yield: 63 % (158 mg, 0.308 mmol); MS (FABMS), *m/z*: 512 $\{M\}^+$ also peaks at 476 $\{M\text{-}Cl\}^+$, 443 $\{M\text{-}2Cl\}^+$;*;* ^{1}H NMR (250 MHz, $CDCl_3$): δ8.1 (4H, d), δ9.0 (4H, d).

Synthesis of [Pt(4-CO_2CH_3-py)$_2$(mnt)] (**3b**) [$PtCl_2$(4-CO_2CH_3-py)$_2$] (120 mg, 0.222 mmol) dissolved in dry DCM (50 mL) and Na_2(mnt) (41.3 mg, 0.222 mmol) in dry MeOH (20 mL) were mixed together and stirred at room temperature for 2 hours under N_2(g). The solvent was reduced to 20 % *in vacuo* (with no heating) and the remaining solution was left overnight in the fridge. The resulting precipitate was collected using filtration. Yield: 41% (55.5 mg, 0.091 mmol); MS (FABMS), *m/z*: 610 $\{M\}^+$ also peaks at 473 $\{M\text{-}py\}^+$; Anal. Calcd for $PtS_2N_4O_4C_{18}H_{14}.2H_2O$; C, 33.48; H, 2.17; N, 8.68. Found: C, 33.69; H, 1.96 ; N, 8.84; ^{1}H NMR (250 MHz, $CDCl_3$): δ8.7 (4H, d), δ7.8 (4H, d), δ3.9 (6H, s). IR (KBr, cm^{-1}): 1730 (s) (C═O stretch), 2203 (s) (C≡N stretch).

Synthesis of [Pt(4-CO_2H-py)$_2$(mnt)] (**3a**) [$PtCl_2$(4-CO_2H-py)$_2$] (119 mg, 0.20 mmol) dissolved in dry DCM (50 mL) and Na_2(mnt) (43 mg, 0.23 mmol) in dry MeOH (20 mL) were mixed together and stirred at room temperature for 2 hours under N_2(g). The solvent was reduced to 20 % *in vacuo* (with no heating), Isopropyl alcohol (50 mL) was added and the mixture was stored in the freezer until a brown precipitate formed. This was collected using filtration and dried under vacuum. Anal. Calcd for $PtS_2N_4O_4C_{18}H_{10}$; C, 33.05; H, 1.72; N, 9.64. Found: C, 32.86; H, 1.83 ; N, 9.43; ^{1}H NMR (250 MHz, DMSO-d6): δ7.5 (4H, d), δ8.5 (4H, d).

X-ray crystallography. Yellow crystals of [$PtCl_2$(4-CO_2CH_3-py)$_2$] were grown by slow evaporation of a DCM / Heptane solution. Crystal, data collection and refinement parameters are summarized in Table 3. Single-crystal X-ray structure determination was carried out using a Smart APEX CCD diffractometer equipped with an Oxford Cryosystems low-temperature device with Mo Kα radiation for data collection. An absorption correction was applied using the multiscan procedure SADABS.[21] The structure was solved by Patterson methods (DIRDIF)[22] and refined using SHELXL.[23] The H-atoms attached to C_{10} were located in a difference synthesis; the CH distances and HCH angles were fixed at ideal values, but the methyl-torsion was refined.

Table 3. Crystallographic Data for $[PtCl_2(4\text{-}CO_2CH_3\text{-}py)_2]$

Chemical formula	$C_{14}H_{14}Cl_2N_2O_4$ Pt	No. indep. refln	2175
Fw	540.26	R(int)	0.0313
T, K	150	$2\theta_{max}$ (deg)	30
Lattice type	monoclinic	*Z*	4
Space group	*C2/c*	D_c, Mg m^{-3}	2.207
a, Å	13.0562(3)	*M*, mm^{-1}	8.978
b, Å	8.2030(2)	Reflects collected	2175
c, Å	15.3120(3)	Parameters	106
β, deg	97.4710(10)	R_1 [$F > 4\sigma(F)$]	0.0182
V, Å^3	1625.99(6)	wR	0.0431
No. reflns for cell	6769	GoF	1.122

Other Experimental Information. All UV/vis spectra were recorded on a Perkin-Elmer Lambda 9 spectrophotometer controlled by a Datalink PC, running UV/Winlab software.

Electrochemical studies were carried out using a DELL GX110 PC with General Purpose Electrochemical System (GPES), version 4.8, software connected to an autolab system containing a PGSTAT 30 or Type III potentiostat. The techniques used a three-electrode configuration, with a 0.5mm diameter Pt disc working electrode, a Pt rod counter electrode and an Ag/AgCl (saturated KCl) reference electrode against which the ferrocenium/ferrocene couple was measured to be +0.55 V. The supporting electrolyte was 0.1 M tetrabutylammonium tetrafluoroborate ($TBABF_4$).

OTTLE (Optically Transparent Thin Layer Electrode) measurements were taken using a quartz cell of 0.5 mm, a Pt/Rh gauze working electrode, an Ag/AgCl reference electrode and a Pt wire counter electrode.[24] UV/vis spectra were recorded on a Perkin-Elmer Lambda 9 spectrophotometer, controlled by a Datalink PC, running UV/Winlab software. Measurements on samples were carried out at 233 K in DMF. $TBABF_4$ (0.1 M) was used as the supporting electrolyte in all cases.

Electron Paramagnetic Resonance spectra were taken using a flat cell, a Pt/Rh gauze working electrode, an Ag/AgCl reference electrode and a Pt wire counter electrode and generated using a BAS CV-27 voltammograph. Spectra were recorded on an X-band Bruker ER200D-SCR spectrometer connected to a Datalink 486DX PC with EPR Acquistion System, version 2.42 software. The temperature was controlled by a Bruker ER4111 VT variable temperature unit. All g values were corrected to 2,2'-diphenyl-1-picrylhydrazyl with $g_{literatue} = 2.0036 \pm 0.0002$.[25] Measurements on samples were carried out at 233 K in DMF. $TBABF_4$ (0.1 M) was used as the supporting electrolyte in all cases.

DFT calculations were run using Gaussian 03, Revision D.01,[26] The images were generated using Arguslab.[27] The 6-31G* basis set was used for the C, N, H, O, Cl and S atoms and the Hay-Wadt VDZ (n+1) ECP basis sets for the Pt(II) centre.[28]

TiO_2 film-covered slides prepared using a previously reported method[29] were treated in the furnace at 300 K for 30 minutes. After allowing to cool to between 50 °C - 100 °C the slides were introduced into an OH bath (pH 11) and left for an hour. The slides were removed from the basic solution and put to dry in the oven at 110 °C for 30 minutes before being introduced into the 0.23 M sensitizing solutions of the dye in MeCN. The prior base treatment of the slides led to the *in situ* hydrolysis and subsequent attachment of the sensitiser dye. The films were removed from the sensitizing solutions after 48 hours and time-resolved kinetics were tested using these sensitised slides covered with a redox inactive electrolyte (0.25 M $LiClO_4$ in propylene carbonate).

Transient absorption decays were measured using the "flash photolysis" technique. The sample was excited with a dye laser (Photon Technology International Inc., GL-301) pumped by a nitrogen laser (Photon Technology International Inc., GL-3300). The excitation wavelength was 450 nm for **3a** dye or 530 nm for **5a** dye. The excitation wavlengths were chosen so the amount of photons absorbed by each dye was comparable. The pulse width was 800 ps, the fluence was about 50 Jcm^{-2} at both excitation wavelengths and the repetition frequency was 1 Hz. A 100-W tungsten-halogen lamp (Bentham, IL1) with a stabilized power supply (Bentham, 605) was used as a probe light source. The probe light passing through the sample was detected with a silicon photodiode (Hamamatsu Photonics, S1722-01). The signal from the photodiode was pre-amplified and sent to the main amplification system with an electronic band-pass filter to improve signal to noise ratio (Costronics Electronics). The amplified signal was collected with a digital oscilloscope (Tektronix, TDS 220), which was synchronized with a trigger signal of the laser pulse from a photodiode (Thorlabs Inc., DET210). To reduce stray light, scattered light and emission from the sample, two monochromators and appropriate optical cut-off filters were placed before and after the sample. Owing to the amplification and noise reduction system, the detectable change of absorbance was as small as 10^{-5} to 10^{-6}.

Notes and references

[1] (a) S. D. Cummings, R. Eisenberg, *J. Am. Chem. Soc.*, 1996, **118**, 1949 (b) J. S. Pap, F. L. Benedito, E. Bothe, E. Bill, S. D. George, T. Weyhermueller, K. Wieghardt, *Inorg. Chem.* 2007, **46**, 4187

[2] J. Zhang, P. Du, J. Schneider, P. Jarosz, R. Eisenberg, *J. Am. Chem. Soc.,* 2007, **129**, 7726

[3] C. Makedonas, C. A. Mitsopoulou, *Eur. J. Inorg. Chem.,* **2006**, 590

[4] J. A. Weinstein, M. T. Tierney, E. S. Davies, K. Base, A. A. Robeiro, M. W. Grinstaff, *Inorg. Chem*., 2006, **45**, 4544

[5] B. O'Regan, M. Grätzel, *Nature*, 1991, **353**, 737; M. Grätzel, *Nature*, 2001, **414**, 338.; N. Robertson, *Angew.Chem. Int. Ed.*, 2006, **45**, 2338

[6] A. Islam, H. Sugihara, K. Hara, L. P. Singh, R. Katoh, M. Yanagida, Y. Takahaski, S. Murata, H. Arakawa, *New J. Chem.*, 2000, **24**, 343

[7] A. Islam, H. Sugihara, K. Hara, L. P. Singh, R. Katoh, M. Yanagida, Y. Takahaski, S.Murata, H. Arakawa, *Inorg. Chem.*, 2001, **40**, 5371

[8] E. A. M. Geary, L. J. Yellowlees, L. A. Jack, I. D. H. Oswald, S. Parsons, N. Hirata, J. R. Durrant, N. Robertson, *Inorg. Chem.*, 2005, **44**, 242

[9] E. A. M. Geary, K. L. McCall, A. Turner, P. R. Murray, E. J. L. McInnes, L. J. Yellowlees, N. Robertson, *Dalton Trans,* **2008**, 3701

[10] C. Yang, J. Qin, Q. Yang, J. Si, S Wang, Y. Wang, P. Ye, C. Ye, *Synth. Mater.*, 2001, **121**, 1491

[11] F. Liu, G. J. Meyer, *Inorg. Chem.,* 2003, **42**, 7351

[12] F. Liu, G. J. Meyer, *Inorg. Chem.,* 2005, **44**, 9305

[13] F. Gajardo, A. M. Leiva, B. Loeb, A. Delgadillo, J. R. Stromberg, G. J. Meyer, *Inorg. Chim. Acta.*, 2008, **361**, 613

[14] P. Qu, G. J. Meyer, *Langmuir*, 2001, **17**, 6720

[15] M. Haga, E. S. Dodsworth, A. B. P. Lever, *Inorg. Chem.,* 1986, **25**, 447

[16] Cambridge Structural Database. *Chem. Des. Autom. News* 1993, **8**, 31.

[17] M. Carnalli, F. Caruso, L. Zambonelli, *Cryst. Struct. Commun.,* 1980, **9**, 721

[18] C. J. Adams, N. Fey, M. Parfitt, S. J. A. Pope and J. A. Weinstein, *Dalton Trans.*, **2007**, 4446.

[19] C. Makedonas and C. A. Mitsopoulou, *Eur. J. Inorg. Chem.*, 2006, 2460; C. Makedonas, C. A. Mitsopoulou, F. J. Lahoz, A. I. Balana, *Inorg. Chem.,* 2003, **42**, 8853; C. Makedonas, C. A. Mitsopoulou, *Inorg. Chim. Acta.,* 2007, **360**, 3997

[20] G. Markl, R. Vybiral, *Tetrahedron Lett.* 1989, **30**, 2903

[21] G. M. Sheldrick, *SADABS. Bruker-AXS* **1997.**

[22] P. T. Beurskens, G. Beurskens, R. de Gelder, S. Garcia-Granda, R. O. Gould, R. Israel, J. M. M. Smits, Crystallography Laboratory, University of Nijmegen, The Netherlands. 1999

[23] G. M. Sheldrick, Institüt für Anorganische Chemie der Universität, Tammanstrasse 4, D-3400 Göttingen, Germany, 1998

[24] S.A. McGregor, E. J. L. McInnes, R. J. Sorbie, L. J. Yellowlees, *Molecular Electrochemistry of Inorganic, Bioinorganic and Organometallic Compounds*; Kluwer: Dordrecht, The Netherlands, 1992

[25] S. A. Al'tshuler, B. M. Kozyrev, *Electronic Paramagnetic Resonance*, Academic Press: New York, **1964**, p 503.

[26] M. J. Frisch, G. W. Trucks, H. B. Schlegel, G. E. Scuseria, M. A. Robb, J. R. Cheeseman, J. A. Montgomery, J. T. Vreven, K. N. Kudin, J. C. Burant, J. M. Millam, S. S. Iyengar, J. Tomasi, V. Barone, B. Mennucci, M. Cossi, G. Scalmani, N. Rega, G. A. Petersson, H. Nakatsuji, M. Hada, M. Ehara, K. Toyota, R. Fukuda, J. Hasegawa, M. Ishida, T. Nakajima, Y. Honda, O. Kitao, H. Nakai, M. Klene, X. Li, J. E. Knox, H. P. Hratchian, J. B. Cross, V. Bakken, C. Adamo, J. Jaramillo, R. Gomperts, R. E. Stratmann, O. Yazyev, A. J. Austin, R. Cammi, C. Pomelli, J. W. Ochterski, P. Y. Ayala, K. Morokuma, G. A. Voth, P. Salvador, J. J. Dannenberg, V. G. Zakrzewski, S. Dapprich, A. D. Daniels, M. C. Strain, O. Farkas, D. K. Malick, A. D. Rabuck, K. Raghavachari, J. B. Foresman, J. V. Ortiz, Q. Cui, A. G. Baboul, S. Clifford, J. Cioslowski, B. B. Stefanov, G. Liu, A. Liashenko, P. Piskorz, I. Komaromi, R. L. Martin, D. J. Fox, T. Keith, M. A. Al-Laham, C. Y. Peng, A. Nanayakkara, M. Challacombe, P. M. W. Gill, B. Johnson, W. Chen, M. W. Wong, C. Gonzalez, J. A. Pople, Gaussian Inc. *Gaussian 03*, Revision D.01; Wallingford CT, 2004.

[27] M. A. Thompson, ArgusLab 4.0.1, Planaria Software LLC, Seattle, WA http://www.arguslab.com

[28] P. J. Hay, W. R. Wadt, *J. Phys. Chem.*, 1985, **82**, 299.

[29] A. N. M. Green, E. Palomares, S. A. Haque, J. M. Kroon, J. R. Durrant, *J. Phys. Chem. B*, 2005, **109**, 12525.